A possible solution of the puzzling variation of the orbital period of MXB 1659-298

R. Iaria,[1]⋆ A. F. Gambino,[1] T. Di Salvo,[1] L. Burderi,[2] M. Matranga,[1] A. Riggio,[2] A. Sanna,[2] F. Scarano,[2] and A. D'Aì[3]

[1]*Dipartimento di Fisica e Chimica, Università di Palermo, via Archirafi 36 - 90123 Palermo, Italy*
[2]*Dipartimento di Fisica, Università degli Studi di Cagliari, SP Monserrato-Sestu, KM 0.7, Monserrato, 09042 Italy*
[3]*INAF/IASF Palermo, via Ugo La Malfa 153, I-90146 Palermo, Italy.*

ABSTRACT
MXB 1659-298 is a transient neutron star Low-Mass X-ray binary system that shows eclipses with a periodicity of 7.1 hr. MXB 1659-298 went to outburst in August 2015 after 14 years of quiescence. We investigate the orbital properties of this source with a baseline of 40 years obtained combining the eight eclipse arrival times present in literature with 51 eclipse arrival times collected during the last two outbursts. A quadratic ephemeris does not fit the delays associated with the eclipse arrival times and the addition of a sinusoidal term with a period of 2.31 ± 0.02 yr is required. We infer a binary orbital period of $P = 7.1161099(3)$ hr and an orbital period derivative of $\dot{P} = -8.5(1.2) \times 10^{-12}$ s s^{-1}. We show that the large orbital period derivative can be explained with a highly non conservative mass transfer scenario in which more than 98% of the mass provided by the companion star leaves the binary system. We predict an orbital period derivative value of $\dot{P} = -6(3) \times 10^{-12}$ s s^{-1} and constrain the companion star mass between ~0.3 and 0.9 ± 0.3 M$_\odot$. Assuming that the companion star is in thermal equilibrium the periodic modulation can be due to either a gravitational quadrupole coupling due to variations of the oblateness of the companion star or with the presence of a third body of mass $M_3 > 21$ Jovian masses.

Key words: X-rays: stars; X-rays: binaries; stars: neutron; binaries: eclipsing; ephemerides; stars: individual (MXB 1659-298)

1 INTRODUCTION

One of the most direct evidence for binary orbital motion is the presence of eclipse of the central source by a companion star. For Low Mass X-ray Binaries (LMXBs) with inclination angles between 75° and 80° the X-ray emission may be totally shielded by the companion star. As the companion transits between the X-ray central source and the observer the light curves show total eclipses. For inclination angles between 80° and 90° the LMXB is observed as an Accretion Disc Corona (ADC) source. In this case the observed X-ray emission comes from an extended corona that can reach the outer region of the accretion disc. The light curves of the ADC sources show an almost sinusoidal modulation and partial eclipses. The modulation of the light curve is generally explained with the presence of a geometrically thick disc whose height varies depending on the azimuthal angle and occults part of the X-ray emission. Since the companion star does not shield the whole extended corona the observed eclipses are partial; the prototype of the ADC sources is X1822-371 (see e.g. Iaria et al. 2011, 2013, 2015a, and references therein).

Total eclipses represent a good time reference, which is ideal to perform timing analysis of the binary orbital period, e.g. the O-C method is usually applied to refine the orbital period or trace orbital period changes (see Chou 2014, for a recent review). To date, 12 LMXBs show total eclipses in their light curve. One of the best studied eclipsing X-ray source is EXO 0748-676, as it was active for more than 20 years (see Wolff et al. 2009, and references therein).

The eclipsing LMXB MXB 1659-298 was discovered by Lewin et al. (1976) in 1976. The light curve showed type-I X-ray bursts, thus revealing that the compact object was an accreting neutron star. The source was observed in outburst up to 1978 with *SAS3* and *HEAO* (Cominsky et al. 1983; Cominsky & Wood 1984, 1989). Eclipses were firstly reported by by Cominsky & Wood (1984), which estimated a periodicity of 7.1 hr. Cominsky & Wood (1989) analysed two whole eclipses estimating two eclipse arrival times. From 1978 up to 1999 the region containing MXB 1659-298 was monitored by the X-ray observatories onboard *Hakucho*, *EXOSAT* and *ROSAT*, but the source was never detected (see Cominsky & Wood 1989; Verbunt 2001). On April 1999 the Wide Field Cameras onboard *BeppoSAX* observed the source in outburst again (in 't Zand et al. 1999). This new outburst continued up to

⋆ E-mail: rosario.iaria@unipa.it

September 2001. During the outburst MXB 1659-298 was observed with the Proportional Counter Array (PCA) onboard *Rossi X-ray Timing Explorer* (*RXTE*, see e.g. Wachter et al. 2000), with the Narrow Field Instruments (NFI) onboard *BeppoSAX* (Oosterbroek et al. 2001) and with *XMM-Newton*. From the analysis of the RXTE light curves of the source, Wachter et al. (2000) obtained four eclipse arrival times and found an orbital period derivative of $(-7.2 \pm 1.8) \times 10^{-11}$ s s^{-1} suggesting that the orbit of the binary system is shrinking. Oosterbroek et al. (2001) obtained two eclipse arrival times from a *BeppoSAX*/NFI observation and combining their data with those present in literature found that the orbital period derivative, $\dot{P}_{\rm orb}$, is positive with a value of $(7.4 \pm 2.0) \times 10^{-12}$ s/s. MXB 1659-298 turned again on outburst on 2015 August 21 (Negoro et al. 2015) and up to 2017 March is still X-ray bright. Using data of the X-ray Telescope (XRT) onboard *Swift*, Bahramian et al. (2016) observed that the unabsorbed flux in the 0.5-10 keV energy range was 1.5×10^{-10}, 4.6×10^{-10} and 2.2×10^{-10} erg cm^{-2} s^{-1} on 2016 January 28, February 2 and 11, respectively.

Cominsky & Wood (1989) measured an eclipse duration, $\Delta T_{\rm ecl}$, of 932±13 s and an ingress/egress duration of $\Delta T_{\rm ing} = 41 \pm 13$ s and $\Delta T_{\rm egr} = 19 \pm 13$ s, respectively. They showed that, if the companion star is a main-sequence star of 0.9 M$_\odot$ with a temperature close to 5000 K, the scale height of the stellar atmosphere should be around 200 km, corresponding to an ingress/egress duration close to 0.5 s. The authors concluded that the small value of the scale height cannot justify the large value of the measured ingress/egress durations. Furthermore, Cominsky & Wood (1989) suggested that the observed asymmetry between the ingress and egress duration could be caused by a one-sided extended corona of size 5×10^5 km.

From the analysis of four eclipses obtained with *RXTE*/PCA, Wachter et al. (2000) estimated an average eclipse duration of 901.9 ± 0.8 s and average values of ingress/egress durations of $\Delta T_{\rm ing} = 9.1 \pm 3.0$ s and $\Delta T_{\rm egr} = 9.5 \pm 3.3$ s. The authors proposed that the large spread of values associated with the ingress/egress times could be caused either by flaring activity of the companion star or by the presence of an evaporating wind from the surface of the companion star created by irradiation from the X-ray source.

Cominsky & Wood (1984) discussed the nature of the optical counterpart of MXB 1659-298, named V2134 Oph, assuming an orbital period of 7.1 hr and an eclipse duration of 900 s. They constrained the mass of the companion star to be between 0.3 M$_\odot$ and 0.9 M$_\odot$ for an inclination angle of the binary system of 90° and 71°.5, respectively. Warner (1995) inferred that the companion star mass is between 0.75 and 0.78 M$_\odot$ if the companion fills its Roche lobe. This range of masses suggests that the companion is a K0 main-sequence star. During the quiescence of MXB 1659-298, Wachter et al. (2000) measured a magnitude in the *I*-band of 22.1 ± 0.3 mag and Filippenko et al. (1999) measured a magnitude in the *R*-band of 23.6 ± 0.4 mag. Wachter et al. (2000) found that the value of $(R - I)_0$ is compatible with an early K spectral type. Moreover, they suggested that, for a companion star belonging to the K0 class, the visual magnitude should be $V = 23.6$ mag, value that is compatible with the measured lower limit of $V > 23$ mag.

Galloway et al. (2008), analysing the type-I X-ray bursts observed with *RXTE*/PCA, inferred a distance to the source of 9±2 and 12 ± 3 kpc for a hydrogen-rich and helium-rich companion star, respectively. Furthermore, Wijnands et al. (2001) detected nearly coherent oscillations with a frequency around 567 Hz during type-I X-ray bursts suggesting that the neutron star could be an X-ray millisecond pulsar with a spin period of 1.8 ms.

The interstellar hydrogen column density, $N_{\rm H}$, was estimated by Cackett et al. (2008) during the X-ray quiescence of MXB 1659-298. Combining *Chandra* and *XMM-Newton* observations collected between 2001 and 2008 they fitted the X-ray spectrum obtaining $N_{\rm H} = (2.0 \pm 0.1) \times 10^{21}$ cm^{-2}. Two more recents *Chandra* observations of the source, taken in 2012 Cackett et al. (2013), seem to suggest an increase of the interstellar hydrogen column density at the value of $(4.7 \pm 1.3) \times 10^{21}$ cm^{-2}. The authors proposed three different scenarios to explain the increase of $N_{\rm H}$: a) material is building up in the outer region of the accretion disc, b) the presence of a precessing accretion disc, and c) sporadic variability during quiescence due to low-level accretion.

Studying the *XMM*-Newton spectrum of MXB 1659-298, Sidoli et al. (2001) detected two absorption lines at 6.64 and 6.90 keV associated with the presence of highly ionised iron (Fe xxv and Fe xxvi ions) as well as absorption lines associated with highly ionised oxygen and neon (O viii 1s-2p, O viii 1s-3p, O viii 1s-4p and Ne ix 1s-2p transition) at 0.65, 0.77, 0.81 and 1.0 keV.

In this paper we report the updated ephemeris of MXB 1659-298 combining 45 eclipse arrival times obtained with *XMM-Newton* and *RXTE* during the outburst between 1999 and 2001 and six eclipse arrival times obtained with *XMM-Newton*, *NuSTAR* and *Swift/XRT* during the outburst started in 2015. The available temporal baseline allows to partially constrain the bizarre behaviour of the eclipse arrival times.

2 OBSERVATIONS

During the outburst occurred from 1999 to 2001, MXB 1659-298 was observed with *XMM-Newton* (Jansen et al. 2001) two times: on March 22 2000 and on Feb. 20 2001. The latter observation (obsid. 0008620701) was analysed by Sidoli et al. (2001) and Díaz Trigo et al. (2006), which studied the spectral properties of the source during the persistent emission, the dip and the eclipse, while the former observation (obsid. 0008620601) was never analysed. During the 2015 outburst, MXB 1659-298 was observed with *XMM-Newton* on September 26, 2015.

The European Photon Imaging Camera (Epic-pn, Strüder et al. 2001) onboard *XMM-Newton* collected data from the source in timing mode, with exposure times of 10, 32 and 34 ks, respectively. The Epic-pn light curve of the observation taken in 2001 shows two eclipses in the light curve (see Fig. 1 in Sidoli et al. 2001). To verify the presence of eclipses in the Epic-pn light curves of the observations taken in 2000 and 2015 we filtered the source events with the Science Analysis System (SAS) ver. 15.0.0. We reprocessed the Epic-pn events and applied the solar-system barycentre corrections adopting as coordinates RA= 255°.527250 and Dec= −29°.945583 (see Wijnands et al. 2003). During the observation taken in 2000, the light curve of MXB 1659-298 shows an eclipse with a duration of 900 s approximately 1400 s after the start time. The count rate is 32 c s^{-1} and 1.4 c s^{-1} outside and during the eclipse, respectively. During the observation taken in 2015, the light curve shows the presence of a type-I X-ray burst at 12 ks after the start of the observation. The count rate varies from 32 c s^{-1} at the beginning of the burst up to 320 c s^{-1} at the peak. An intense dipping activity is present at about 20 ks from the beginning of the observation, a complete eclipse is observed at 26 ks from the start time and an eclipse without the ingress is observed at beginning of the observation. The count rate out and during the eclipse is 32 and 1.4 c s^{-1}, respectively.

The PCA instrument onboard *RXTE* (Jahoda et al. 1996) observed several times the source from 1999 to 2001. In our analysis we selected 43 *RXTE*/PCA observations showing the eclipse and
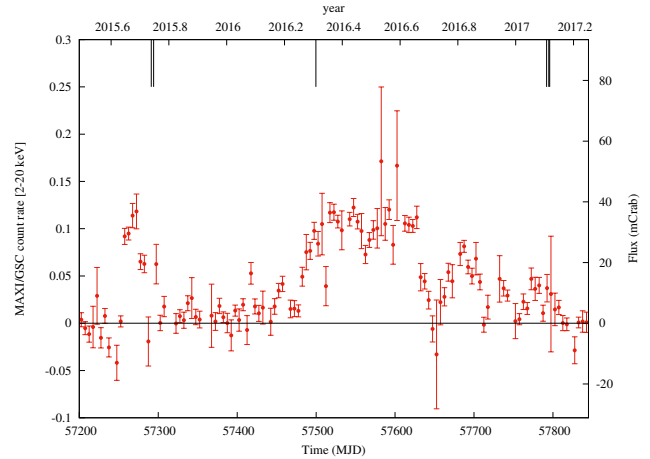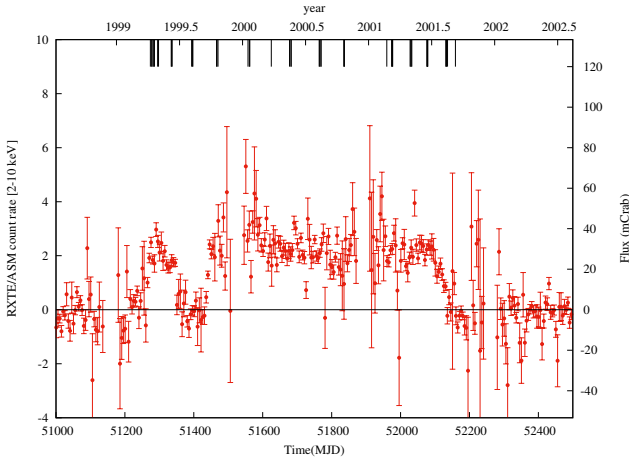
Figure 1. Light curve of MXB 1659-298 during the outburst occurred between 1999 and 2001 (left panel) and the latest started 2015 (right panel). The left panel shows the RXTE/ASM light curve in the 2-10 keV, the right panel shows the MAXI/GSC light curve in the 2-20 keV energy range; the bin time is **five days** for both the light curves. The eclipse arrival times are also indicated.

for which it is possible to estimate the ingress and egress time accurately. To estimate the eclipse arrival times from the *RXTE*/PCA observations we analysed the standard product background-subtracted light curves with a bin time of 0.125 s and we applied the solar-system barycentric correction to the events using the ftool `faxbary`.

NuSTAR (Harrison et al. 2013) observed MXB 1659-298 two times in 2015 and 2016 with both the independent solid state photon counting detector modules (FPMA and FPMB), with elapsed times of 96 ks and 50 ks, respectively. We processed the raw (Level 1) data with the ftool `nupipeline` (Heasoft ver. 6.19), obtaining cleaned and calibrated event data (Level 2). The solar-system barycentric corrected events of the FPMA and FPMB telescopes have been obtained applying the tool `nuproducts` on the Level 2 data. The corresponding light curves were created selecting a circular extraction region for the source events with a radius of 49″ and using the 1.6-20 keV energy range. The persistent emission has a count rate of 2 c s^{-1}. A complete eclipse and an eclipse without the ingress are observed at 24 and 76 ks from the start time. The count rate during the eclipse is 0.02 c s^{-1}. It is also evident the presence of the ingress to the eclipse at 49.7 ks from the start time. During the second observation MXB 1659-298 is brighter, with a persistent count rate of 20 c s^{-1}, a whole eclipse is observed 30 ks after the start time of the observation. To increase the statistics of the *NuSTAR* light curve we summed the FPMA and FPMB light curve using the ftool `lcmath`.

During the 2015 outburst, MXB 1659-298 was observed several times with *Swift*/XRT (Gehrels et al. 2004; Burrows et al. 2005), although only three observations show a complete eclipse. We obtained further *Swift*/XRT data as target of opportunity observations performed on February 8, 10 and 11, 2017 (obsid 0003400266, 0003400267 and 0003400268). All of the three observations cover the whole eclipse. The XRT data were processed with standard procedures (xrtpipeline v0.13.1), and with standard filtering and screening criteria with ftools. For our timing analysis, we also converted the event arrival times to the solar-system barycentre with the tool `barycorr` and subtracted the background using the ftool `lcmath`.

The All Sky monitor (ASM, Levine et al. 1996) onboard *RXTE* monitored the 1999-2001 outburst (Fig. 1, left panel). The two *XMM-Newton* observations were performed at a similar ASM count rate of 2.5 c s^{-1} (about 30 mCrab in flux), corresponding to the source maximum flux. The outburst showed a sort of precursor last-
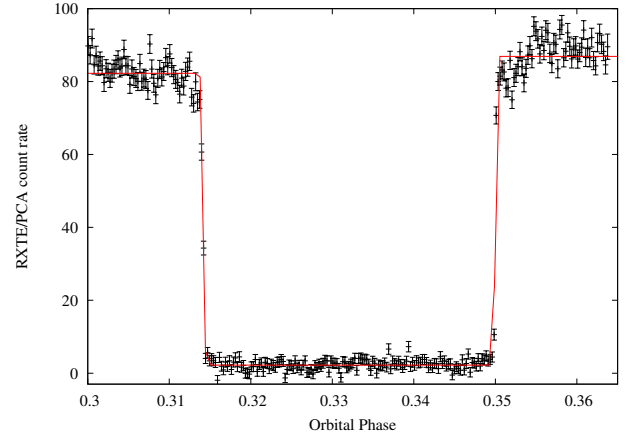
Figure 2. Eclipse of MXB 1659-628 observed by the RXTE/PCA instrument (observation P40050-04-16-00). The superimposed red function is the step-and-ramp function adopted to estimate the eclipse arrival time.

ing 100 d, afterwards the flux decreased up to a value compatible with zero for 86 d, and finally increased again rapidly reaching a constant flux of 30 mCrab for 700 d.

The Gas Slit Camera (GSC, Mihara et al. 2011) onboard the Monitor of All-sky X-ray Image (MAXI, Matsuoka et al. 2009) observed the recent outburst (see Fig. 1, right panel). The morphology of the outburst is similar to the previous one with a sort of precursor lasting 50 d, a new quiescent stage lasting 150 d and, after that, an increase of the flux at 30 mCrab lasting 150 d. The maximum GSC count rate is 0.12 c s^{-1}. *XMM-Newton* and *NuSTAR* (obsid. 90101013002) observed the source when the GSC count rate was 0.05 c s^{-1}; *NuSTAR* observed the source a second time when MXB 1659-298 was brighter with a corresponding GSC count rate of 0.1 c s^{-1}.

3   METHOD AND ANALYSIS

To estimate the eclipse arrival times, we folded the solar-system barycentric corrected light curves using a trial time of reference and orbital period, T_{fold} and P_0, respectively. The value of the adopted

Table 1. Journal of the X-ray eclipse arrival times of MXB 1659-298

Point	Eclipse Time (MJD;TDB)	Cycle	Delay (s)	Ref.	Point	Eclipse Time (MJD;TDB)	Cycle	Delay (s)	Ref.
1	43 058.7260(2)	0	0(13)	[1],[2]	31	51 769.43726(2)	29378	107.0(1.3)	[4]
2	43 574.6441(2)	1740	26(13)	[1],[2]	32	51 835.261275(9)	29600	106.9(7)	[3]
3	51 273.978079(2)	27707	96.46(13)	[2]	33	51 836.447292(6)	29604	106.8(5)	[3]
4	51 274.571102(8)	27709	97.7(7)	[3]	34	51 837.040274(5)	29606	104.4(4)	[3]
5	51 277.832626(4)	27720	95.4(3)	[2]	35	51 960.08961(2)	30021	101(2)	[3]
6	51 278.425648(10)	27722	96.5(9)	[3]	36	51 974.321836(6)	30069	101.4(5)	[3]
7	51 281.687174(4)	27733	94.5(3)	[2]	37	51 974.914836(8)	30071	100.6(7)	[3]
8	51 283.762726(3)	27740	96.2(3)	[2]	38	51 976.397381(8)	30076	102.5(6)	[3]
9	51 285.838220(11)	27747	93.0(9)	[3]	39	51 977.286855(12)	30079	99.1(1.0)	[3]
10	51 295.029855(5)	27778	92.5(4)	[3]	40	52 027.692627(9)	30249	99.2(7)	[3]
11	51 297.698476(8)	27787	99.4(7)	[3]	41	52 029.768118(8)	30256	95.8(7)	[3]
12	51 334.464970(12)	27911	93.6(1.1)	[3]	42	52 030.954185(12)	30260	100.0(1.1)	[3]
13	51 335.650973(6)	27915	92.2(5)	[3]	43	52 032.733167(8)	30266	96.1(7)	[3]
14	51 337.133479(6)	27920	90.8(5)	[3]	44	52 076.615786(4)	30414	91.7(3)	[3]
15	51 393.46935(4)	28110	92(4)	[3]	45	52 077.208801(7)	30416	92.2(6)	[3]
16	51 396.13784(4)	28119	87(3)	[3]	46	52 077.801847(6)	30418	95.3(5)	[3]
17	51 397.32378(3)	28123	81(3)	[3]	47	52 078.394837(7)	30420	93.7(6)	[3]
18	51 466.112958(9)	28355	91.5(8)	[3]	48	52 078.987831(8)	30422	92.4(7)	[3]
19	51 467.29898(12)	28359	92.2(1.0)	[3]	49	52 131.469068(10)	30599	86.8(9)	[3]
20	51 470.264016(9)	28369	91.1(8)	[3]	50	52 132.65509(2)	30603	87(2)	[3]
21	51 557.436333(6)	28663	89.8(5)	[3]	51	52 133.24811(8)	30605	88(7)	[3]
22	51 561.290937(6)	28676	93.7(5)	[3]	52	52 136.50958(8)	30616	81(7)	[3]
23	51 562.477008(6)	28680	98.3(5)	[3]	53	52 159.34046(2)	30693	83.9(1.4)	[3]
24	51 625.03951(2)	28891	104(2)	[3]	54	57 291.24010(2)	48001	17(2)	[3]
25	51 677.817305(4)	29069	101.3(4)	[3]	55	57 294.20513(2)	48011	16(2)	[3]
26	51 681.671901(6)	29082	104.5(5)	[3]	56	57 499.682737(14)	48704	13.7(1.2)	[3]
27	51 682.857903(7)	29086	103.2(6)	[3]	57	57 792.03631(3)	49690	23(3)	[3]
28	51 763.803676(5)	29359	106.3(4)	[3]	58	57 794.70484(5)	49699	22(4)	[3]
29	51 764.989711(8)	29363	107.7(7)	[3]	59	57 795.89087 (5)	49703	23(4)	[3]
30	51 768.84426(2)	29376	106.0(1.4)	[4]					

NOTE — Epoch of reference 43 058.72595 MJD, orbital period 7.11610872 hr, the associated errors are at 68% confidence levels; [1] Cominsky & Wood (1989), [2] Wachter et al. (2000), [3] this work, [4] Oosterbroek et al. (2001) .
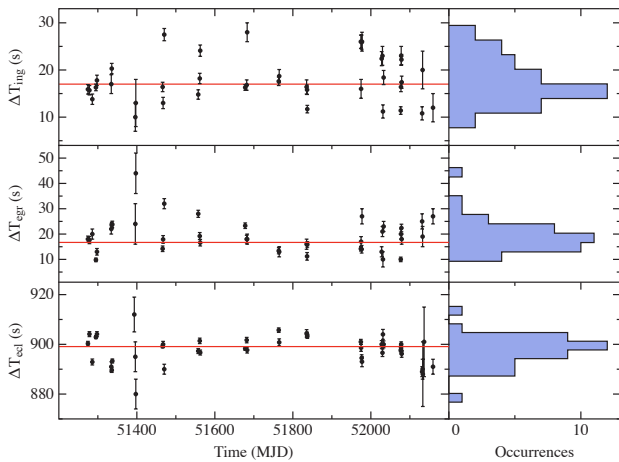
Figure 3. From the top-left to the bottom-left the ingress, egress and eclipse duration, respectively, as function of time. The values are obtained from the RXTE/PCA eclipses analysed in this work. The red lines indicate the average values for each duration. From the top-right to the bottom-right we show the histograms of the occurrences of the ingress, egress and eclipse duration.

T_{fold} corresponds to a time close to the start time of the corresponding observation. The adopted value of P_0 is 7.11610872 hr corresponds to the value of the orbital period at T_0 = 43 058.72609

MJD obtained by Oosterbroek et al. (2001) adopting quadratic ephemeris.

We fitted the eclipse profiles with a simple model consisting of a step-and-ramp function, where the count rates before, during, and after the eclipse are constant and the intensity changes linearly during the eclipse transitions. This model involves seven parameters: the count rate before, during, and after the eclipse, called C_1, C_2, and C_3, respectively; the phases of the start and stop times of the ingress (ϕ_1 and ϕ_2), and, finally, the phases of the start and stop times of the egress (ϕ_3 and ϕ_4). We show a typical eclipse of MXB 1659-298 in Fig. 2. The eclipse was observed during the RXTE/PCA observation P40050-04-16-00, the superimposed red function is the step-and-ramp best-fitting function. The phase corresponding to the eclipse arrival time ϕ_{ecl} is estimated as $\phi_{ecl} = (\phi_2 + \phi_3)/2$. The corresponding eclipse arrival time is given by $T_{ecl} = T_{fold} + \phi_{ecl}P_0$. To be more conservative, we scaled the error associated with ϕ_{ecl} by the factor $\sqrt{\chi^2_{red}}$ to take into account values of χ^2_{red} of the best-fit model larger than one. We show the obtained eclipse arrival times in Barycentric Dynamical Time (TDB), in units of MJD, in Tab. 1.

We used the 43 RXTE/PCA observations to estimate the average duration, ΔT_{ecl}, ΔT_{ing} and ΔT_{egr} of the eclipse, the ingress and the egress, respectively. The values of ΔT_{ecl}, ΔT_{ing} and ΔT_{egr} for each eclipse are shown as function of the eclipse arrival times in Fig. 3. We found that ΔT_{ecl} is scattered between 890 and 910 s. Fitting the values of eclipse duration with a constant we obtained a $\chi^2(d.o.f.)$ of 561(42) and a best-fit value of $\Delta T_{ecl} = 899.1 \pm 0.6$ s at 68%

Table 2. Best-fit values

Parameter	LQ	LQS	LQCS
a (s)	-109 ± 38	65 ± 20	9 ± 29
b (s d^{-1})	0.046 ± 0.007	0.015 ± 0.004	0.037 ± 0.009
c ($\times 10^{-6}$ s d^{-2})	-2.6 ± 0.3	-1.2 ± 0.2	-4.0 ± 1.1
d ($\times 10^{-10}$ s d^{-3})	-	-	1.0 ± 0.4
A (s)	-	9.6 ± 0.6	10.2 ± 0.7
P_{mod} (d)	-	843 ± 7	855 ± 8
t_ϕ (d)	-	137 ± 75	-7 ± 82
χ^2(d.o.f.)	4083(56)	512(53)	455(52)
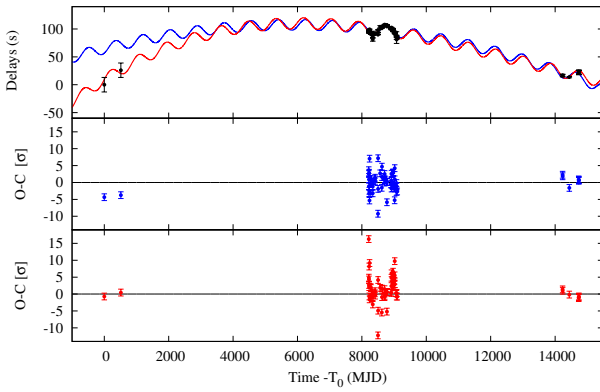
Figure 4. Top panel: delays with respect to the predicted eclipse arrival times, assuming as epoch of reference T_0 = 43 058.72595 MJD and as orbital period P_0 = 7.11610872 hr, plotted versus time. The blue and red curves indicate the best-fit functions corresponding to eqs. 2 and 4, respectively. Middle panel: residuals in units of σ with respect to the blue curve. Bottom panel: residuals in units of σ with respect to the red curve.

confidence level (c.l.). The ingress duration is scattered between 10 and 30 s while the egress duration is scattered between 10 and 35 s. Fitting the ingress duration values with a constant we obtained a $\chi^2(d.o.f.)$ of 457 (38) and a best-fit value of $\Delta T_{\mathrm{ing}} = 17.0 \pm 0.7$ s at 68% c. l., while, fitting the egress duration values we obtained a $\chi^2(d.o.f.)$ of 560 (39) and a best-fit value of $\Delta T_{\mathrm{egr}} = 16.7 \pm 0.9$ s at 68% c. l.. The associated errors were scaled by the factor $\sqrt{\chi^2_{\mathrm{red}}}$ to take a value of χ^2_{red} of the best-fit model larger than one into account. We find that the average duration of the ingress and egress are similar. We also show in Fig. 3 the occurrences of the measured ingress, egress and duration using a bin of 3.1, 3.7 and 3.5 s, respectively.

We calculated the delays with respect to P_0 = 7.11610872 hr and to a reference epoch of T_0 = 43 058.72595 MJD, corresponding to the first eclipse arrival time obtained by Cominsky & Wood (1989). The inferred delays, in units of seconds, of the eclipse arrival times with respect to a constant orbital period are reported in Tab. 1. For each point we computed the corresponding cycle and the eclipse arrival time in days with respect to the adopted T_0. We show the delays vs. time in Fig. 4 (top panel).

Initially we fitted the delays with a quadratic function

$$y(t) = a + bt + ct^2, \tag{1}$$

where t is the time in days (MJD-43 058.72595), $a = \Delta T_0$ is the correction to T_0 in units of seconds, $b = \Delta P/P_0$ in units of s d^{-1} with

ΔP the correction to the orbital period, and finally, $c = 1/2 \ \dot{P}/P_0$ in units of s d^{-2}, with $\dot{P}$ representing the orbital period derivative. The corresponding best-fitting parameters are shown in the LQ column of Tab. 2. With a χ^2 of 4083 for 56 d.o.f., we note that the quadratic function does not acceptably fit the data. Since the delays seem to show a periodic modulation we fitted them using the function

$$y(t) = a + bt + ct^2 + A \sin\left[\frac{2\pi}{P_{\mathrm{mod}}}(t - t_\phi)\right], \tag{2}$$

where A is the amplitude in seconds of the sinusoidal function, P_{mod} is the period of the sine function in days, and, finally, t_ϕ represents the time in days at which the sinusoidal function is null. A clear improvement is obtained with a value of χ^2(d.o.f.) of 512 (53) that translates to a F-test probability chance improvement of 7×10^{-24}. The best-fit function, indicated with a blue curve, and the corresponding residuals are shown in the top and middle panels of Fig. 4. The best-fit values are shown in the third column of Tab. 2. The corresponding ephemeris (hereafter LQS) is

$$T_{\mathrm{ecl}}(N) = \mathrm{MJD(TDB)} \ 43\,058.7267(2) + 0.296504580(13)N -$$
$$1.3(2) \times 10^{-12}N^2 + A \sin\left[\frac{2\pi}{N_{\mathrm{mod}}}N - \phi\right], \tag{3}$$

where N indicates the number of cycles, $N_{\mathrm{mod}} = P_{\mathrm{mod}}/P_0$ and $\phi = 2\pi t_\phi/P_{\mathrm{mod}}$. We obtained an orbital period derivative $\dot{P} = -8.5(1.2) \times 10^{-12}$ s s^{-1}, a sinusoidal modulation characterised by a periodicity $P_{\mathrm{mod}} = 2.31 \pm 0.02$ yr and a semiamplitude $A = 9.6 \pm 0.6$ s.

It is evident that the LQS ephemeris does not predict the first two eclipse arrival times. A possible explanation is that the orbital period derivative is changing from 1976 up to now. To take into account this fact, we added a cubic term to eq. 2, defining the new function

$$y(t) = a + bt + ct^2 + dt^3 + A \sin\left[\frac{2\pi}{P_{\mathrm{mod}}}(t - t_\phi)\right], \tag{4}$$

where d includes the presence of a derivative of $\dot{P}$ with $d \simeq \ddot{P}/(6P)$. With the latter model we obtain a value of χ^2(d.o.f.) of 455 (52). By adding the cubic term we find a F-test probability chance improvement of 0.014 indicating that the improvement of the fit is between two and three σ of confidence level. The best-fit function, indicated with a red curve, and the corresponding residuals are shown in the top and bottom panel of Fig. 4. The best-fit parameters are shown in the fourth column of Tab. 2. The corresponding ephemeris (hereafter LQCS) is

$$T_{\mathrm{ecl}}(N) = \mathrm{MJD(TDB)} \ 43\,058.7261(3) + 0.296504566(3)N -$$
$$4.0(1.1) \times 10^{-12}N^2 + 3.0(1.2) \times 10^{-17}N^3 +$$
$$A \sin\left[\frac{2\pi}{N_{\mathrm{mod}}}N - \phi\right], \tag{5}$$

from which we inferred the orbital period derivative at time T_0 = 43 058.7261 MJD to be $\dot{P} = -2.7(7) \times 10^{-11}$ s s^{-1} and the orbital period second derivative $\ddot{P} = 2.4(9) \times 10^{-20}$ s s^{-2}. The sinusoidal modulation has a period of $P_{\mathrm{mod}} = 2.34 \pm 0.02$ yr and a semiamplitude of $A = 10.2 \pm 0.7$ s.

4 DISCUSSION

We analysed the eclipse arrival times of MXB 1659-298 with the main aim to estimate its ephemeris. Our baseline spans 40 years and covers the three outbursts of the source observed from 1976.

We combined 51 eclipse arrival times, corresponding to the outbursts occurred in 1999-2001 and in 2015-2017, with the data already reported in literature. The campaign of observations made with *Rossi-XTE*/PCA during the 1999-2001 outburst seems to indicate a possible periodic modulation of 2.3 years; the delays associated with the six eclipse arrival times obtained during the most recent outburst agree with that periodic modulation. We find that the LQS ephemeris accounts for the eclipse arrival times except for the two eclipses observed in 1976-1978. The addiction of a cubic term (LQCS ephemeris) allows to account for all the available data, however the statistical improvement is less than three sigma, suggesting that a larger baseline is needed to confirm the more complex ephemerides. In both cases, a sinusoidal modulation with a period between 840 and 860 days is needed to obtain an acceptable fit of the eclipse arrival times. In the following we restrict our discussion to the LSQ ephemeris.

To estimate the eclipse arrival times we fitted the shape of the eclipse using a step-and-ramp function. We used the *RXTE*/PCA observations, covering 2.4 years during the second outburst of MXB 1659-298, to estimate the ingress/egress and eclipse durations. The obtained values are scattered, the mean values associated with the eclipse, ingress and egress are $\Delta T_{\rm ecl} = 899.1 \pm 0.6$ s, $\Delta T_{\rm ing} = 17.0 \pm 0.7$ s and $\Delta T_{\rm egr} = 16.7 \pm 0.9$ s, respectively. We find that the ingress and egress durations are similar contrarily to what reported by Cominsky & Wood (1989), that obtained an ingress and egress duration of 41 ± 13 s and 19 ± 13 s, respectively. Our different results can be explained by the larger sample and the higher quality of our dataset.

The ingress, egress, and eclipse durations show a jittered behaviour of the order of 15 s similarly to what observed in EXO 0748-676 (Wolff et al. 2002). Wolff et al. (2007) discussed the possibility that magnetic activity of the companion star generates extended coronal loops above the photosphere that could explain the amplitude of the observed jitter. This scenario may be plausible given the late K or early M type nature of the 0.3-0.4 $M_\odot$ companion star in EXO 0748-676. Such stars can have magnetic activity if they rotate and if they have significant convective envelopes (see Wolff et al. 2007). The companion star in MXB 1659-298 is an early K type main-sequence star (see below), and hence it likely has similar magnetic activity. Ponti et al. (2017) showed that AX J1745.6-2901 has a different phenomenology. Although jitters are observed in the ingress and egress, the eclipse duration is nearly constant. The authors suggested that the matter ejected from the accretion disc could reach the companion star with a ram pressure comparable to the pressure in the upper layers of the companion star (that is a K type main-sequence star). This interaction could displace the atmosphere of the companion star delaying both the ingress and the egress times.

4.1   The masses of the binary system

We can estimate the companion star radius from the size of its Roche lobe, that can be expressed by using the formula of Paczyński (1971)

$$R_{\rm L_2} = 0.462a \left(\frac{m_2}{m_1 + m_2} \right)^{1/3}, \qquad (6)$$

where a is the orbital separation of the binary system and m_1 is the neutron star mass in units of solar masses. Combining the previous equation with the third Kepler's law we find that

$$R_{\rm L_2} = 0.233 \, m_2^{1/3} P_{\rm h}^{2/3} R_\odot. \qquad (7)$$

Assuming that the companion star fills its Roche lobe then the radius of the companion star R_2 coincides with $R_{\rm L_2}$. To estimate the mass of the companion star we adopted the mass-radius relation for a companion star in thermal equilibrium obtained by studying the cataclysmic variable systems (eq. 16 in Knigge et al. 2011) although LMXBs lie in a somewhat different region of parameter space. We adopted the relation valid for large orbital periods that is

$$R_2 = 0.293 \pm 0.010 \left(\frac{M_2}{M_{\rm conv}} \right)^{0.69 \pm 0.03} R_\odot, \qquad (8)$$

where $M_{\rm conv}$ has a value of $0.20 \pm 0.02 \, M_\odot$ and it is the mass of the convective region of the companion star. Combining the eqs. 7 and 8 and taking into account that the accuracy associated with the Roche lobe radius is 2% we find that the companion star has a mass of $0.9 \pm 0.3 \, M_\odot$ and a radius of $0.84 \pm 0.10 \, R_\odot$. Hereafter we will assume a neutron star mass of $1.48 \pm 0.22 \, M_\odot$, this mass value was estimated by Özel et al. (2012) analysing the mass distribution of neutron stars that have been recycled; the best value is the mean of the distribution and the associated error is the corresponding dispersion.

4.2   The mass accretion rate and the mass transfer rate

Using RXTE/PCA data taken during the outburst in 1999, Galloway et al. (2008) observed that the flux of MXB 1659-298 peaked at $\sim 1.0 \times 10^{-9}$ erg s^{-1} cm^{-2} in the 2-25 keV energy range during April 1999 , but it was between 4×10^{-10} and 6×10^{-10} erg s^{-1} cm^{-2} throughout the remainder of the outburst. To infer a good estimation of the flux in the 0.1-100 keV energy band, we adopted the broadband best-fit model of the persistent spectrum obtained by Oosterbroek et al. 2001, from which we extrapolate an unabsorbed flux of 1.0×10^{-9} erg s^{-1} cm^{-2}.

From the analysis of the type-I X-ray bursts the distance to MXB 1659-298 was estimated to be 9 ± 2 and 12 ± 3 kpc for a hydrogen-rich and helium-rich companion star, respectively (see Galloway et al. 2008). We assume the average of the two values, $d = 11 \pm 4$ kpc, considering that the source is accreting mixed H/He (Galloway et al. 2008).

To convert the X-ray luminosity in mass accretion rate we used the relation $L_x = \gamma \dot{M}_{\rm acc} c^2$, where γ is the efficiency of the accretion and c is the speed of the light. We take into account that the neutron star is rapidly spinning with a frequency of 567 Hz (Wijnands et al. 2001) adopting the relation proposed by Sibgatullin & Sunyaev (2000)

$$\gamma = 0.213 - 0.153 f_{\rm kHz} + 0.02 f_{\rm kHz}^2, \qquad (9)$$

where $f_{\rm kHz}$ is the spin frequency of the neutron star in units of kHz. The latter relation is valid assuming a gravitational mass of the neutron star of 1.4 $M_\odot$ and the commonly adopted FPS equation of state for a neutron star. Using a spin frequency of 567 Hz we find that $\gamma \simeq 0.132$. Our assumption implies that all of the released gravitational energy is converted to X-ray emission and that negligible amount of energy is carried away by bulk outflows. This is confirmed by the spectral studies of the source; in fact, the absorption lines associated with the presence of Fe xxv and Fe xxvi ions are narrow suggesting that it is not possible to associate to the source a superluminal jet (see Sidoli et al. 2001). Furthermore Díaz Trigo & Boirin (2016) suggested that MXB 1659-298 could have a mild thermal wind but only static atmospheres have been reported.

Using $\gamma \simeq 0.132$ we find $\dot{M}_{\rm acc} = (2.0 \pm 1.5) \times 10^{-9} \, M_\odot$ yr^{-1}. Considering a quiescence duration of almost 14.5 yr and a mean outburst duration of 1.5 yr we find that the average value of the

observed mass accretion rate is $|\langle \dot{M}_{\rm acc}\rangle| \simeq \dot{M}_{\rm acc}1.5/16 = (1.9 \pm 1.4)\times 10^{-10}$ M$_\odot$ yr^{-1}.

On the other hand, from theoretical considerations, we can estimate the rate of mass that has to be transferred from the companion star in order to explain the quadratic term of the LQS ephemeris interpreted as the orbital period derivative of the system. From the long-term orbital evolution we can estimate the mass transfer rate $\dot{M}_2$ using the eq. 4 in Burderi et al. (2010)

$$\dot{m}_{-8} = 35(3n-1)^{-1}m_2\left(\frac{\dot{P}_{-10}}{P_{\rm 5h}}\right), \tag{10}$$

where $\dot{m}_{-8}$ is the mass transfer rate $\dot{M}_2$ in units of 10^{-8} M$_\odot$ yr^{-1}, n is the mass-radius index of the companion star, m_2 is the companion star mass in units of solar masses, $\dot{P}_{-10}$ is the orbital period derivative in units of 10^{-10} s s^{-1} and $P_{\rm 5h}$ is the orbital period in units of 5 hr. This is derived combining the third Kepler law with the contact condition, that is $\dot{R}_{\rm L2}/R_{\rm L2} = \dot{R}_2/R_2$ (where $\dot{R}_{\rm L2}$ is the Roche Lobe radius of the secondary and R_2 is the radius of the secondary). Adopting $n = 0.69 \pm 0.03$, $m_2 = 0.9 \pm 0.3$, $\dot{P} = -8.5(1.2)\times 10^{-12}$ s s^{-1} and $P = 7.1161099(3)$ hr, we find that the mass transfer rate implied by the observed orbital period derivative is $\dot{M}_2 = -(1.8 \pm 0.7)\times 10^{-8}$ M$_\odot$ yr^{-1}, that is almost two orders of magnitude higher that the observed averaged mass accretion rate. This means that in order to explain the observed orbital period change rate we have to invoke a highly not conservative mass transfer for this system.

The above described scenario assumes a mass transfer rate of $\dot{M}_2 = -(1.8 \pm 0.7)\times 10^{-8}$ M$_\odot$ yr^{-1} and a companion star mass of 0.9 ± 0.3 M$_\odot$ in thermal equilibrium. The time scale associated with the mass transfer rate, $\tau_{\rm M} = M_2/|\dot{M}_2|$, is $(5 \pm 3) \times 10^7$ yr. The companion star is in thermal equilibrium if $\tau_{\rm M}$ is longer than the thermal time scale $\tau_{\rm KH} = GM_2^2/(R_2 L_2)$ of the companion star (Paczyński 1971). To estimate the thermal timescale we need to infer the luminosity L_2 of the companion star. For a star close to the lower main sequence it holds the relation $L_2/L_\odot = (M_2/M_\odot)^4$ (see Salaris & Cassisi 2005). For a companion star mass of 0.9 ± 0.3 M$_\odot$ we obtain that $\tau_{\rm KH} = (5 \pm 3)\times 10^7$ yr which is comparable with $\tau_{\rm M}$, for this reason we cannot exclude the the companion star is less massive of 0.9 ± 0.3 M$_\odot$.

4.3 The prediction of the orbital period derivative for a highly non conservative mass transfer

We can define a parameter β in the following way, $-\dot{M}_1 = \beta \dot{M}_2$, where $\dot{M}_1 = |\langle \dot{M}_{\rm acc}\rangle|$ is the mass accretion rate. Hence $\beta = 1$ in a conservative mass transfer scenario and $\beta < 1$ in a non conservative mass transfer scenario. Comparing the observed averaged mass accretion rate with the mass transfer rate implied by the observed orbital period derivative, we obtain $\beta = 0.011 \pm 0.009$, suggesting that only $\sim 1\%$ of the mass transferred from the companion star is indeed accreted onto the neutron star.

According to the orbital evolution theory, orbital period changes are expected to be driven by mass transfer from the companion to the compact object, by emission of gravitational waves (GR) and/or by magnetic braking (MB). For orbital periods larger than two hours the effects of MB dominate the orbital evolution of the binary system. Following Verbunt & Zwaan (1981), Verbunt (1993) and Tauris (2001) the torque associated with MB can be parametrised as

$$T_{\rm MB} = 8.4(k^2)_{0.1}f^{-2}m_1^{-1}P_{\rm 2h}^2 q^{1/3}(1+q)^{2/3}, \tag{11}$$

where f is a dimensionless parameter for which a value of either 0.79 (Skumanich 1972) or 1.78 (Smith 1979) has been assumed, $k = 0.323$ is the gyration radius for a star with mass of 0.8 M$_\odot$ (Claret & Gimenez 1990), $P_{\rm 2h}$ is the orbital period in units of two hours, q is the mass ratio M_2/M_1 and, finally, m_1 is the mass of the compact object in units of solar masses. Because $T_{\rm MB}$ depends on f^{-2} the effects of the MB on the derivative of the angular momentum of the binary system will be larger for $f = 0.79$ than for $f = 1.78$.

We can calculate the secular orbital period derivative expected from the non-conservative secular evolution of the system using the relation

$$\dot{P}_{-12} = 1.37q(1+q)^{-1/3}m_1^{5/3}P_{\rm 2h}^{-5/3}\left[\frac{1/3-n}{2g(\alpha,\beta,q)-1/3+n}\right]\times$$
$$[1+T_{\rm MB}], \tag{12}$$

where

$$g(\alpha,\beta,q) = 1 - \beta q - \frac{1-\beta}{1+q}\left(\frac{q}{3}+\alpha\right) \tag{13}$$

(see Di Salvo et al. 2008; Burderi et al. 2009, 2010), where $\dot{P}_{-12}$ is the orbital period derivative in units of 10^{-12} s s^{-1} and α is a dimensionless parameter that quantifies the specific angular momentum of the ejected matter in the case of a non-conservative mass transfer scenario. The specific angular momentum, $l_{\rm ej}$, with which the transferred mass is lost from the system can be written in units of the specific angular momentum of the secondary, that is $\alpha = l_{\rm ej}/(\Omega_{\rm orb}r_2^2) = l_{\rm ej}P(M_1+M_2)^2/(2\pi a^2 M_1^2)$, where r_2 is the distance of the secondary star from the centre of mass of the system, a is the orbital separation and P is the orbital period of the binary system. For a neutron star mass of 1.48 ± 0.22 M$_\odot$ we obtain an orbital period derivative of $-(6 \pm 3)\times 10^{-12}$ s s^{-1}, which is compatible within one σ with the value $\dot{P} = -(8.5 \pm 1.2)\times 10^{-12}$ s s^{-1} inferred from the eclipse arrival times.

A highly non-conservative mass transfer in this source may be justified by the fact that MXB 1659-298 is a fast spinning neutron star (Wijnands et al. 2001). During the quiescent periods, if the region around the neutron star is free from matter up to the light cylinder radius, the radiation pressure of the rotating magnetic dipole, given by the Larmor formula, may be able to eject from the system the matter transferred by the companion star at the inner Lagrangian point, according to the mechanism termed *radio ejection* and described in detail in Burderi et al. (2001). Once significant temporary reduction of the mass accretion rate occurs, the neutron star can emit as a magnetic-dipole rotator and the radiation pressure from the pulsar may be able to eject the matter transferred from the companion out of the system. We note that the disc instability model (see the review of Lasota 2001) may have a role in triggering the *radio ejection* and starting a non conservative mass transfer. The *radio ejection* has been invoked to explain the high orbital period derivative observed in the accreting millisecond pulsar (AMSP) SAX J1808.4-3658 (see Di Salvo et al. 2008; Burderi et al. 2009), and, more recently, for the AMSP SAX J1748.9-2021 for which a high orbital period derivative is also observed (Sanna et al. 2016). We therefore suggest that a similar mechanism could be also at work for MXB 1659-298.

The above described scenario assumes a mass transfer rate of $\dot{M}_2 = -(1.8 \pm 0.7)\times 10^{-8}$ M$_\odot$ yr^{-1} and a companion star mass of 0.9 ± 0.3 M$_\odot$. The time scale associated with the mass transfer rate, $\tau_{\rm M} = M_2/|\dot{M}_2|$, is $(5.1 \pm 2.7)\times 10^7$ yr. The companion star is in thermal equilibrium if $\tau_{\rm M}$ is longer than the thermal time scale $\tau_{\rm KH} = GM_2^2/(R_2 L_2)$ of the companion star (Paczyński 1971). To

estimate the thermal timescale we need to infer the luminosity L_2 of the companion star. For a star close to the lower main sequence it holds the relation $L_2/L_\odot = (M_2/M_\odot)^4$ (see Salaris & Cassisi 2005). Since the companion star mass is 0.9 ± 0.3 M$_\odot$ we obtain that $\tau_{KH} = (5 \pm 3) \times 10^7$ yr which is comparable with τ_M. Since the two timescales are comparable we cannot exclude that the companion star is out of the thermal-equilibrium; hence, the value of 0.9 ± 0.3 M$_\odot$ has to be considered an upper limit to the companion star mass.

We note that for a mass of the companion star lower than $0.9 M_\odot$ the mass transfer rate would be also lower, because of the linear dependence of $\dot{M}_2$ on m_2 in eq. 10. Therefore, the minimum mass transfer rate is reached for a $m_2 = 0.35$ M$_\odot$. This has to be considered as a lower limit to the mass of the companion since below this mass the companion star is expected to become fully convective and the magnetic braking switches off (Rappaport et al. 1983). For this limiting mass, the mass transfer rate is $(7 \pm 3) \times 10^{-9}$ M$_\odot$ yr^{-1}. However, a detailed study of the evolution of this system is beyond the aims of this paper and will be reported elsewhere. Here we note that the results presented in this paper do not change significantly adopting a lower mass for the companion star. Therefore, we will continue our discussion assuming a companion star mass of 0.9 ± 0.3 M$_\odot$, keeping in mind that lower masses for the companion star are also possible.

4.3.1 The changes of the equivalent hydrogen column density N_H during the X-ray quiescence

The mass ejected from the system can explain the variable equivalent hydrogen column density N_H measured during the X-ray quiescence of the source. Cackett et al. (2008, 2013) measured two different N_H values of $(2.0 \pm 0.1) \times 10^{21}$ cm^{-2} and $(4.7 \pm 1.3) \times 10^{21}$ cm^{-2}, respectively, at different times, while the estimation of N_H obtained by Dickey & Lockman (1990) is 1.8×10^{21} cm^{-2}. Here we suggest that the matter ejected from the system can account for the additional absorption. Most of the matter provided by the companion is ejected from the inner Lagrangian point forming a circumbinary ring of matter around MXB 1659-298. Because of the large inclination angle of the system it is possible that the ejected matter interposes between the source and the observer. Local density inhomogeneities and/or changes in the mass transfer rate could produce changes in the equivalent hydrogen column as observed by Cackett et al. (2008, 2013) during quiescence.

We use the eq. 4 of Iaria et al. (2013) to estimate the density of the ejected matter

$$n(r) \simeq 6.9 \times 10^{11} (1-\beta)\zeta^{-1}\eta^{-1}\dot{m}_E(m_1+m_2)^{-1}P_h^{-1}\left(\frac{r}{a}\right)^{-3/2},$$
(14)

where $n(r)$ is the density in units of cm^{-3}, r is the distance from the inner Lagrangian point, ζ is a parameter that takes into account a non-spherical distribution of matter, η a parameter larger than 1, $\dot{m}_E$ is the mass transfer rate in units of Eddington mass accretion rate and a is the orbital separation of the binary system. Adopting a mass transfer rate of $|\dot{M}_2| = (1.8 \pm 0.7) \times 10^{-8}$ M$_\odot$ yr^{-1}, an orbital period of 7.116 hr, a companion star mass and a neutron star mass of 0.9 ± 0.3 M$_\odot$ and 1.48 ± 0.22 M$_\odot$, respectively, we obtain $n(a) = (5 \pm 2) \times 10^{10}(\zeta\eta)^{-1}$ cm^{-3}. Supposing a constant particle density along the line of sight, we can determine the equivalent hydrogen column density N_H associated with the neutral matter using $N_H = n(a) \times a$, where $a = (1.74 \pm 0.10) \times 10^{11}$ cm. We find

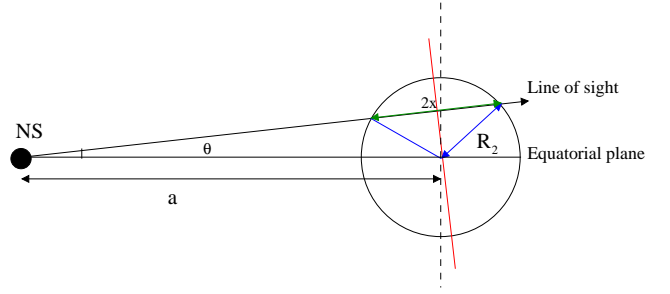**Figure 5.** Schematic geometry of MXB 1659-298 not in scale.

$N_H = (8 \pm 4) \times 10^{21}(\zeta\eta)^{-1}$ cm^{-2}. Since the quantity $\zeta\eta$ is close to unity (see Iaria et al. 2013) we find that the equivalent hydrogen column of the cold matter is $N_H = (8 \pm 4) \times 10^{21}$ cm^{-2}, that is of the same order of magnitude of the changes observed during quiescence of the source and, furthermore, it explains the discrepancy by a factor of two between the N_H values measured by Cackett et al. (2013) and Dickey & Lockman (1990).

4.3.2 The inclination angle of the source

From our estimate of the duration of the eclipse ingress, that is $\Delta T_{ing} \simeq 17$ s, we can estimate the size of the corona, R_c, surrounding the central source using the relation

$$\frac{2\pi}{P}a = \frac{2R_c}{\Delta T_{ing}},$$
(15)

we find $R_c = (3.6 \pm 0.3) \times 10^8$ cm. Assuming a neutron star mass of 1.48 ± 0.22 M$_\odot$ and a companion star mass of 0.9 ± 0.3 M$_\odot$ we infer that the Roche lobe radius, R_{L_1} of the compact object is 5.8×10^{10} cm. The radius of the accretion disc, R_d, corresponds to the tidal radius $R_T \simeq 0.9 R_{L_1}$ (see Frank et al. 2002, eq. 5.122), hence the accretion disc radius is $R_d \simeq 5.3 \times 10^{10}$ cm. This result suggests that the corona is much smaller than the accretion disk, and therefore it is a relatively compact corona around the neutron star.

Using our estimate of the eclipse duration we can also estimate the inclination angle, $i = 90° - \theta$, of the system finding the angle θ represented in Fig. 5. Knowing that the eclipse duration is $\Delta T_{ecl} \simeq 899.1$ s we can estimate the size of the occulted region x as before using

$$\frac{2\pi}{P}a = \frac{2x}{\Delta T_{ecl}}.$$
(16)

We obtain $x = (1.92 \pm 0.11) \times 10^{10}$ cm, where $2x$ is the green segment shown in Fig. 5. The angle θ, representing the angle between the line of sight and the equatorial plane of MXB 1659-298, is obtained from

$$\tan\theta = \left[\frac{R_2^2 - x^2}{a^2 - (R_2^2 - x^2)}\right]^{1/2}.$$

We infer $i = 72 \pm 3$ degrees. Our result is compatible with the presence in the light curve of the source of dips and total eclipses that can be observed for inclination angles in the approximate range $75°$–$80°$ (see Fig. 5.10 in Frank et al. 2002). We note that for a companion star mass of 0.35 M$_\odot$ the inclination angle of the system is 76.0 ± 0.7 degree, that is marginally compatible with the value obtained for a companion star mass of 0.9 ± 0.3 M$_\odot$.

Sidoli et al. (2001) detected absorption lines associated with the presence of O VIII, Ne IX, Fe XXV and Fe XXVI ions in the XMM

spectrum of MXB 1659-298. The authors, assuming an inclination angle of 80° inferred the distance of the absorbing plasma from the central source, finding $r_{\rm Fe} \lesssim 2.4 \times 10^8$ cm, $r_{\rm O} \gtrsim 3 \times 10^8$ cm and $r_{\rm Ne} \gtrsim 9 \times 10^7$ cm, respectively. Revisiting the results obtained by Sidoli et al. (2001) for an inclination angle of 72° we find $r_{\rm Fe} \lesssim 8 \times 10^8$ cm, $r_{\rm O} \gtrsim 1 \times 10^9$ cm and $r_{\rm Ne} \gtrsim 3 \times 10^8$ cm. Since we have estimated a size of the corona of $R_{\rm c} \simeq 3.6 \times 10^8$ cm, we suggest that the absorbing plasma is located in the outer regions of the corona.

4.4 The 2.31-yr periodic modulation: possible explanations

Our ephemeris of MXB 1659-298 also includes a sinusoidal modulation with a period of 2.31 ± 0.02 yr. One possibility is that this periodic modulation observed in the delays may be produced by the gravitational coupling of the orbit with changes in the shape of the magnetically active companion star. These changes are thought to be the consequence of the torque applied by the magnetic activity of a sub-surface magnetic field in the companion star with the convective envelope. The convective envelope induces a cyclic exchange of angular momentum between the inner and outer regions of the companion star causing a change in the gravitational quadrupole moment (see Applegate 1992; Applegate & Shaham 1994). A similar mechanism has been proposed for the eclipsing LMXBs EXO 0748-676 (Wolff et al. 2009) and AX J1745.6-2901 (Ponti et al. 2017).

The inferred periodicity of 843 d and the amplitude of 9.6 s correspond in this case to an orbital period variation of $\Delta P/P = (8.3 \pm 0.5) \times 10^{-7}$. We estimate that the transfer of angular momentum needed to produce an orbital period change ΔP is $\Delta J \simeq 3.8 \times 10^{46}$ g cm^2 s^{-1} (see Applegate 1992, eq. 27). The asynchronism of the companion, quantified through the quantity $\Delta\Omega/\Omega$, is 3.7×10^{-4}, where Ω is the orbital angular velocity of the binary system and $\Delta\Omega$ is the variation of the orbital angular velocity needed to produce ΔP (see Applegate & Shaham 1994, eq. 3). The variable part of the luminosity of the companion star required to power the gravitational quadrupole changes is $\Delta L \simeq 1.5 \times 10^{32}$ erg s^{-1}. Considering that $L_2/L_\odot = (M_2/M_\odot)^4$ we obtain $\Delta L/L_2 = 0.06 \pm 0.10$, in agreement with the prediction of $\Delta L \simeq 0.1L$ obtained for magnetic active stars (see Applegate 1992, and references therein). Our results suggest that a change in the magnetic quadrupole of the companion star can produce the observed sinusoidal modulation. The energy required to transfer the angular momentum from the interior of the companion star to a thin shell, with a mass of 10% of M_2, at the surface (and viceversa) is furnished by ten percentage of the thermonuclear energy produced by the companion star. Furthermore, we obtain that the mean sub-surface magnetic field B of the companion star is close to 1×10^5 G (see Applegate 1992, eq. 23).

The origin of the sinusoidal modulation could also be explained by the presence of a third body orbiting around the binary system, similarly to what is found for the LMXB XB 1916-053 (Iaria et al. 2015b). Adopting the inclination angle of 72°.1 we find that the orbital separation between the centre of mass of MXB 1659-298 and the centre of mass of the triple system is $a_{\rm x} \sin i = A\,c$, where c is the speed of light. Using the values in the third column of Tab. 2 we obtain that $a_{\rm x} \sin i = (2.9 \pm 0.2) \times 10^{11}$ cm. Assuming a non-eccentric and coplanar orbit of the third body and that the companion star is in thermal equilibrium, the mass M_3 of the third body is obtained from

$$\frac{M_3 \sin i}{(M_3 + M_{\rm bin})^{2/3}} = \left(\frac{4\pi^2}{G}\right)^{1/3} \frac{Ac}{P_{\rm mod}^{2/3}}, \qquad (17)$$

where $M_{\rm bin}$ is the mass of the binary system and $P_{\rm mod}$ is the rev-

olution period of the third body around the binary system (see e.g. Bozzo et al. 2007). We obtain that the mass of the third body is 22 ± 3 M_J, where M_J indicates the Jovian mass; the distance of the third body from the centre of mass of the triple system is 2.3 ± 0.3 AU. Releasing the constrain of a co-planar orbit the mass of the third body is larger than 21 M_J. We have checked that the derived orbit of the third body is stable in the formalism by Kiseleva et al. (1994). If this result will be confirmed, this will be the first circumbinary Jovian planet spotted around a LMXB. In the case of a no-coplanar orbit we find that the mass of the third body should be larger than 21 M_J.

5 CONCLUSIONS

We have estimated 51 eclipse arrival times for MXB 1659-298 when the source was in outburst in 2000, 2001 and 2015 using *Rossi-XTE*, *XMM-Newton*, *NuSTAR* and *Swift/XRT* data. Combining these times to the previous ones reported in literature we obtain a baseline of 40 years, from 1976 to 2017, to constrain the ephemeris of the source. The data are clustered in three temporal intervals covering six years corresponding to the periods when the source was in outburst. In the hypothesis that the companion star is in thermal equilibrium and fills its Roche Lobe, we estimate that the companion star mass is 0.9 ± 0.3 $M_\odot$, in agreement with the possibility that the companion is an early K-type main-sequence star as reported in literature.

Using RXTE/PCA data we have studied the profile of the total eclipse observing jitters in the ingress/egress duration and eclipse duration of about 10-15 s. The average values of the ingress, egress and eclipse durations are 17.0 ± 0.7 s, 16.7 ± 0.9 s and 899.1 ± 0.6 s, respectively. Using the average ingress and eclipse duration values we find that the size of the corona surrounding the neutron star is $R_{\rm c} = (3.6 \pm 0.3) \times 10^8$ cm and the inclination angle of the binary system is 72 ± 3 degree assuming a companion star in thermal equilibrium.

We find that the eclipse arrival times are well described by ephemeris composed of a linear, a quadratic and a sinusoidal term. We find an orbital period derivative of $\dot{P} = -8.5(1.2) \times 10^{-12}$ s s^{-1}. We are able to explain the value of $\dot{P}$ assuming a highly non conservative mass transfer scenario. We find that the mass transfer rate is $\dot{M}_2 = -(1.8 \pm 0.7) \times 10^{-8}$ $M_\odot$ yr^{-1}, and only 1% of this mass is observed to accrete onto the neutron star. We also suggest that the ejected matter produces a local absorber with an equivalent hydrogen column density of $(8 \pm 4) \times 10^{21}$ cm^{-2}.

The sinusoidal modulation has a period of 2.31 ± 0.02 yr and an amplitude of 9.6 ± 0.6 s. The 2.3-yr periodic modulation of the orbital period can be explained either with the presence of a gravitational quadrupole coupling of the orbit to a variable deformation of the magnetically active companion star or with the presence of a third body orbiting around the binary system. In the second scenario we find that the mass of the third body is larger than 21 M_J.

Finally, we note that the first two eclipse arrival times, measured during the outburst occurred in 1976-1978, are marginally accounted for the quadratic ephemeris. To fit them we adopted a more complex ephemeris taking into account the second derivative of the orbital period. However, the statistical improvement is smaller than three σ. A larger baseline is needed to confirm or discard more complex ephemerides.

ACKNOWLEDGEMENTS

REFERENCES

Applegate J. H., 1992, ApJ, 385, 621
Applegate J. H., Shaham J., 1994, ApJ, 436, 312
Bahramian A., Heinke C. O., Wijnands R., Degenaar N., 2016, The Astronomer's Telegram, 8699
Bozzo E., et al., 2007, A&A, 476, 301
Burderi L., et al., 2001, ApJ, 560, L71
Burderi L., Riggio A., di Salvo T., Papitto A., Menna M. T., D'Aì A., Iaria R., 2009, A&A, 496, L17
Burderi L., Di Salvo T., Riggio A., Papitto A., Iaria R., D'Aì A., Menna M. T., 2010, A&A, 515, A44
Burrows D. N., et al., 2005, Space Sci. Rev., 120, 165
Cackett E. M., Wijnands R., Miller J. M., Brown E. F., Degenaar N., 2008, ApJ, 687, L87
Cackett E. M., Brown E. F., Cumming A., Degenaar N., Fridriksson J. K., Homan J., Miller J. M., Wijnands R., 2013, ApJ, 774, 131
Chou Y., 2014, Research in Astronomy and Astrophysics, 14, 1367
Claret A., Gimenez A., 1990, Ap&SS, 169, 215
Cominsky L. R., Wood K. S., 1984, ApJ, 283, 765
Cominsky L. R., Wood K. S., 1989, ApJ, 337, 485
Cominsky L., Ossmann W., Lewin W. H. G., 1983, ApJ, 270, 226
Di Salvo T., Burderi L., Riggio A., Papitto A., Menna M. T., 2008, MNRAS, 389, 1851
Díaz Trigo M., Boirin L., 2016, Astronomische Nachrichten, 337, 368
Díaz Trigo M., Parmar A. N., Boirin L., Méndez M., Kaastra J. S., 2006, A&A, 445, 179
Dickey J. M., Lockman F. J., 1990, ARA&A, 28, 215
Filippenko A. V., Leonard D. C., Matheson T., Li W., Moran E. C., Riess A. G., 1999, PASP, 111, 969
Frank J., King A., Raine D. J., 2002, Accretion Power in Astrophysics: Third Edition
Galloway D. K., Muno M. P., Hartman J. M., Psaltis D., Chakrabarty D., 2008, ApJS, 179, 360
Gehrels N., et al., 2004, ApJ, 611, 1005
Harrison F. A., et al., 2013, ApJ, 770, 103
Iaria R., di Salvo T., Burderi L., D'Aí A., Papitto A., Riggio A., Robba N. R., 2011, A&A, 534, A85
Iaria R., Di Salvo T., D'Aì A., Burderi L., Mineo T., Riggio A., Papitto A., Robba N. R., 2013, A&A, 549, A33
Iaria R., et al., 2015a, A&A, 577, A63
Iaria R., et al., 2015b, A&A, 582, A32
Jahoda K., Swank J. H., Giles A. B., Stark M. J., Strohmayer T., Zhang W., Morgan E. H., 1996, in Siegmund O. H., Gummin M. A., eds, Proc. SPIEVol. 2808, EUV, X-Ray, and Gamma-Ray Instrumentation for Astronomy VII. pp 59–70, doi:10.1117/12.256034
Jansen F., et al., 2001, A&A, 365, L1
Kiseleva L. G., Eggleton P. P., Orlov V. V., 1994, MNRAS, 270, 936
Knigge C., Baraffe I., Patterson J., 2011, ApJS, 194, 28
Lasota J.-P., 2001, New Astron. Rev., 45, 449
Levine A. M., Bradt H., Cui W., Jernigan J. G., Morgan E. H., Remillard R., Shirey R. E., Smith D. A., 1996, ApJ, 469, L33
Lewin W. H. G., Hoffman J. A., Doty J., Liller W., 1976, IAU Circ., 2994
Matsuoka M., et al., 2009, PASJ, 61, 999
Mihara T., et al., 2011, PASJ, 63, S623
Negoro H., et al., 2015, The Astronomer's Telegram, 7943
Oosterbroek T., Parmar A. N., Sidoli L., in't Zand J. J. M., Heise J., 2001, A&A, 376, 532
Özel F., Psaltis D., Narayan R., Santos Villarreal A., 2012, ApJ, 757, 55
Paczyński B., 1971, ARA&A, 9, 183
Ponti G., De K., Muñoz-Darias T., Stella L., Nandra K., 2017, MNRAS, 464, 840
Rappaport S., Verbunt F., Joss P. C., 1983, ApJ, 275, 713
Salaris M., Cassisi S., 2005, Evolution of Stars and Stellar Populations
Sanna A., et al., 2016, MNRAS, 459, 1340
Sibgatullin N. R., Sunyaev R. A., 2000, Astronomy Letters, 26, 699
Sidoli L., Oosterbroek T., Parmar A. N., Lumb D., Erd C., 2001, A&A, 379, 540
Skumanich A., 1972, ApJ, 171, 565
Smith M. A., 1979, PASP, 91, 737
Strüder L., et al., 2001, A&A, 365, L18
Tauris T. M., 2001, in Podsiadlowski P., Rappaport S., King A. R., D'Antona F., Burderi L., eds, Astronomical Society of the Pacific Conference Series Vol. 229, Evolution of Binary and Multiple Star Systems. p. 145 (arXiv:astro-ph/0012077)
Verbunt F., 1993, ARA&A, 31, 93
Verbunt F., 2001, A&A, 368, 137
Verbunt F., Zwaan C., 1981, A&A, 100, L7
Wachter S., Smale A. P., Bailyn C., 2000, ApJ, 534, 367
Warner B., 1995, Cataclysmic Variable Stars. Cambridge Astrophysics, Cambridge University Press
Wijnands R., Strohmayer T., Franco L. M., 2001, ApJ, 549, L71
Wijnands R., Nowak M., Miller J. M., Homan J., Wachter S., Lewin W. H. G., 2003, ApJ, 594, 952
Wolff M. T., Hertz P., Wood K. S., Ray P. S., Bandyopadhyay R. M., 2002, ApJ, 575, 384
Wolff M. T., Wood K. S., Ray P. S., 2007, ApJ, 668, L151
Wolff M. T., Ray P. S., Wood K. S., Hertz P. L., 2009, ApJS, 183, 156
in 't Zand J., Heise J., Smith M. J. S., Cocchi M., Natalucci L., Celidonio G., Augusteijn T., Freyhammer L., 1999, IAU Circ., 7138

This paper has been typeset from a TEX/LATEX file prepared by the author.